






SHORT COMMUNICATION



Discovery of a new class of triazole based inhibitors of acetyl transferase KAT2A

Roberta Pacifico^a, Nunzio Del Gaudio^b, Guglielmo Bove^b, Lucia Altucci^b , Lydia Siragusa^c, Gabriele Cruciani^d, Menotti Ruvo^e , Rosa Bellavita^f , Paolo Grieco^f  and Mauro F. A. Adamo^a 

^aCentre for Synthesis and Chemical Biology (CSCB), Department of Chemistry, Royal College of Surgeons in Ireland, Dublin, Ireland;

^bDepartment of precision medicine, University of Campania Luigi Vanvitelli, Naples, Italy; ^cMolecular Horizon Srl, Bettona, Italy; ^dLaboratory for Chemometrics and Molecular Modeling, Department of Chemistry, Biology, and Biotechnology, University of Perugia, Perugia, Italy; ^eInstitute of Biostructures and Bioimaging, Consiglio Nazionale delle Ricerche, Naples, Italy; ^fDepartment of Pharmacy, School of Medicine, University of Naples 'Federico II', Naples, Italy

ABSTRACT

We have recently developed a new synthetic methodology that provided both *N*-aryl-5-hydroxytriazoles and *N*-pyridine-4-alkyl triazoles. A selection of these products was carried through virtual screening towards targets that are contemporary and validated for drug discovery and development. This study determined a number of potential structure target dyads of which *N*-pyridinium-4-carboxylic-5-alkyl triazole displayed the highest score specificity towards KAT2A. Binding affinity tests of abovementioned triazole and related analogs towards KAT2A confirmed the predictions of the *in-silico* assay. Finally, we have run *in vitro* inhibition assays of selected triazoles towards KAT2A; the ensemble of binding and inhibition assays delivered pyridyl-triazoles carboxylates as the prototype of a new class of inhibitors of KAT2A.

ARTICLE HISTORY

Received 26 May 2022
Revised 23 June 2022
Accepted 28 June 2022

KEYWORDS

N-pyridine triazoles; KAT2A inhibitors; virtual screening; acetyl transferases; anti-cancer

1. Introduction



1,2,3-triazoles are commonly recognised as important chemical scaffolds as well as efficient molecules in the area of medicinal chemistry^{1,2}. Given their versatile behaviour in acting as both Lewis acids and bases^{3,4}, triazoles have been used as a core structural motif in a huge variety of drug classes such as: anti-microbial^{5,6}, anti-inflammatory⁷, antineoplastic⁸, antiviral⁹, anti-hypertensive¹⁰ or as immunomodulatory agents¹¹.


We have recently reported a novel synthetic pathway that, by reacting β -ketoesters **1** and azides **2**, provided 1,2,3-triazoles **3** or **4** (Scheme 1). The reactions employing 2-unsubstituted β -ketoesters were found to provide 5-methyl-1,2,3-triazoles **4**; whereas 2-alkyl-substituted β -ketoesters provided 5-hydroxy 1,2,3-triazoles **3** in high yields and as a single regioisomer¹².

As a follow up of this work, we have posed the question of whether or not those classes of new compounds may be useful in medicinal chemistry. Triazoles were repeatedly reported as bio-active compounds^{1–11} and many drug candidates containing the pyridine ring were equally described. Pyridines are commonly used in medicinal chemistry because of their ability to establish hydrogen bonds either as donors or acceptors, their water solubility, small dimensions and, most importantly, their potential to act as amide bioisosteres¹³. The latter in particular, makes pyridine pivotal in drug discovery¹⁴. Additionally, if compared to the benzene ring^{15–17}, the pyridine unit displays a relevant increased basicity¹⁸, an improved aqueous solubility¹⁹ and a smaller polar surface²⁰; all of these features consent an optimal orientation of the pyridine-containing drugs with the biological target through π -stacking interactions^{21,22}. According to the FDA²³, there are

more than 95 approved drugs containing the pyridine moiety that are, currently, employed against tuberculosis (i.e., isoniazid^{24,25} **5** and ethionamide²⁶ **6**), HIV/AIDS (i.e., delavirdine²⁷ **7**), Alzheimer disease (i.e., tacrine²⁸ **8**), Raynaud's syndrome (i.e., nifedipine²⁹ **9**), hypertension (e.g., nivaldipine³⁰ **10**) and so on among the others (Figure 1).

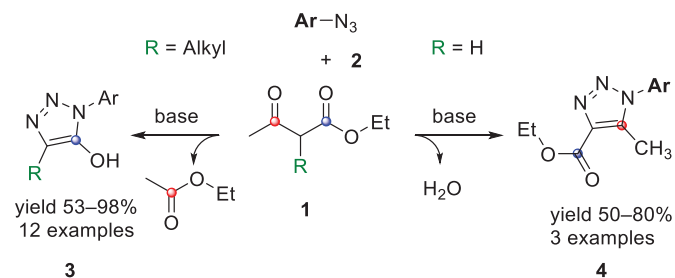
In order to answer the research question on new triazoles' bio-activity, we submitted a small selection of pyridine-based compounds **11–18** (Figure 2) into a virtual screening study, which identified in *N*-(pyridin-2-yl)-4-carboxylic-5-methyl triazole **16** (Figure 2) a new chemical template with significant activity and selectivity as KAT2A inhibitor. KAT2A, also known as GCN5 (general control nonderepressible 5), is part of the HAT (histone acetyltransferase) family and, more specifically, belongs to the GCN5-related *N*-acetyltransferase group^{31,32}. KAT2A promotes the acetylation of the ϵ -amino group of lysines thus preventing the positive charge on the amino group to impact other proteins interaction. Furthermore, the neutralisation of lysine positive charge leads to a weaker bond with DNA strands allowing transcriptional factors to penetrate DNA itself more easily³³. Dysregulation of KATs' activity is associated with numerous severe tumours such as small-cell lung cancer³⁴ or colon cancer³⁵, inflammatory disorders³⁶, type 2 diabetes³⁷ and so on. So far, only few HATs inhibitors are available and have been approved for therapeutic use (Figure 3). They mainly derive from natural sources such as anacardic acid³⁸ **19**, garcinol^{39,40} **20** or curcumin⁴¹ **21** even though synthetic products, bearing thiazole⁴² **22**, isothiazole^{43,44} **23** and pyrido/benzothiazolone⁴⁵ **24** units, have been

CONTACT Mauro F. A. Adamo  madamo@rcsi.ie  Centre for Synthesis and Chemical Biology (CSCB), Department of Chemistry, Royal College of Surgeons in Ireland, Dublin, Ireland

 Supplemental data for this article is available online at <https://doi.org/10.1080/14756366.2022.2097447>.

© 2022 The Author(s). Published by Informa UK Limited, trading as Taylor & Francis Group.

This is an Open Access article distributed under the terms of the Creative Commons Attribution License (<http://creativecommons.org/licenses/by/4.0/>), which permits unrestricted use, distribution, and reproduction in any medium, provided the original work is properly cited.



Scheme 1. Preparation of triazoles **3** and **4**.

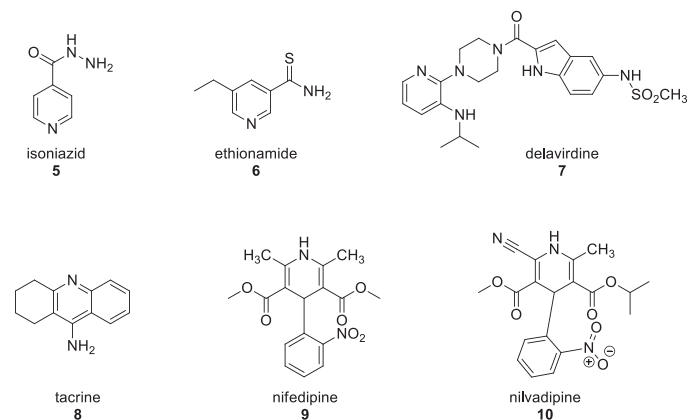


Figure 1. Few examples of approved drugs containing a pyridine unit.

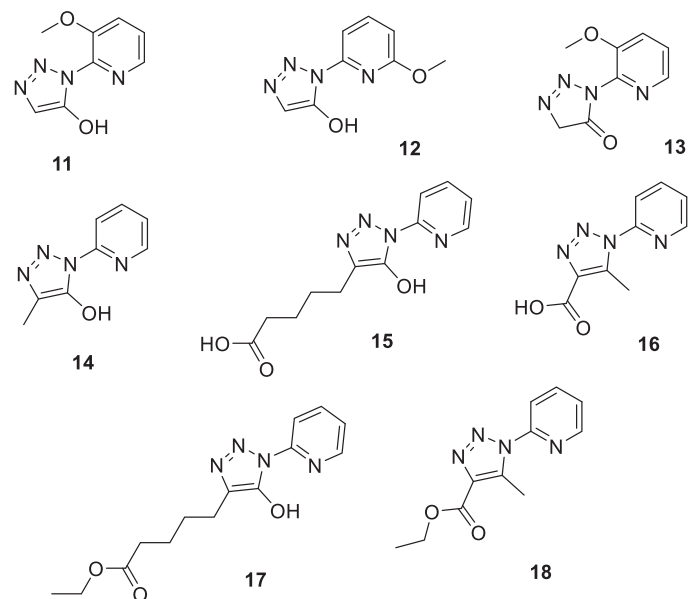


Figure 2. Pyridine-based triazoles tested through docking screening against the BioGPS cavity database.

recently introduced and proved to have a higher activity and specificity compared to the natural products.

Unfortunately, most of the HATs inhibitors known showed lack of selectivity towards members of the HAT family and, therefore, selectivity for a specific enzyme, for example, KAT2A, is still an outstanding issue.

Herein we describe each stage of our research that led to the identification of compound **16** (Figure 2) as a new KAT2A inhibitor

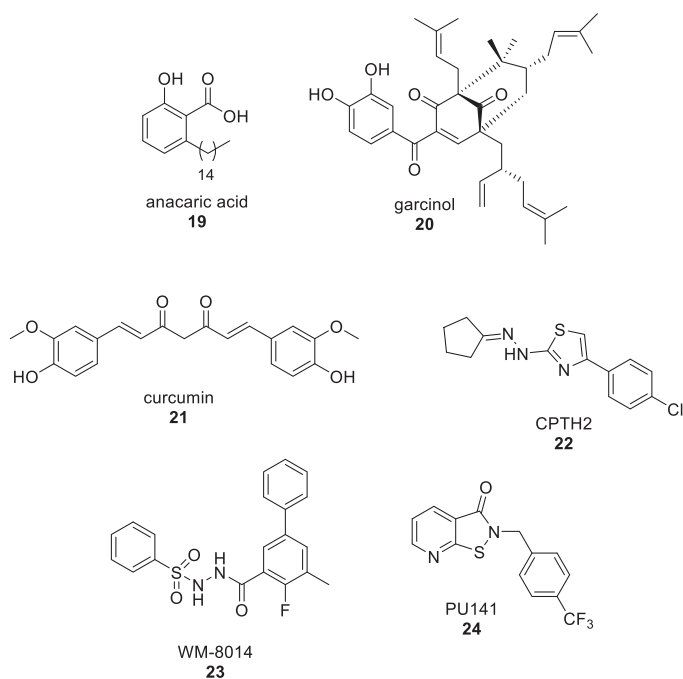


Figure 3. Natural and synthetic HATs inhibitors.

template. This study includes virtual screening, synthesis, binding studies and *in vitro* testing.

2. Results and discussion

2.1. Virtual screening

Compounds **11–18** were submitted to virtual screening towards a database of proteins with established structure and role in system biology using the BioGPS software in combination with the FLAP algorithm. The BioGPS workflow used for the docking screening of triazoles **11–18** consisted in 5 parts: i) Protein refinement, achieved by using an algorithm known as “Fixpdb” that enables the preparation of the protein structure obtained from the Protein Data Bank (PDB)⁴⁶; ii) Cavity detection, achieved by using an algorithm known as “Flapsite” that allows for the identification of pocket points located within a distance of 4 Å maximum from the closest protein⁴⁶; iii) and iv) Cavity characterisation and comparison, achieved by the FLAP algorithm (Fingerprints for Ligands And Proteins) that enables the identification of the potential complementary ligand pharmacophoric features for a protein binding site^{46,47}; v) Data analysis, in which each pocket/target similarity is analysed by using the global scores that attribute to 0 no similarity and to 1 maximum similarity⁴⁶. This study provided docking results and score distribution of **11–18** versus the protein panel (Table 1)⁴⁶. Importantly each of the proteins listed in Table 1 is a significant target for medicinal chemistry as for example KAT2A^{31–37}.

The results collated in Table 1 report the following: (1) numbers are arbitrary scores comprised between 1 and 100 and reflect the fitting of molecules **11–18** to the enzyme pocket; (2) red cells indicate a bad ligand-protein fitting; (3) green cells indicate medium ligand-protein fitting meanwhile (4) blue cells indicate a good ligand protein fitting. The results obtained showed the following: (i) triazoles **11–14**, bearing a hydroxyl group at position C5, did not show significant binding scores (Table 1, except for Rab7a⁴⁸ and Serine/Threonine- protein phosphatase 5 (PP5)⁴⁹; (ii)

Table 1. Docking scores for triazoles 11–18 found for this dataset of twenty proteins.

Protein name	11	12	13	14	15	16	17	18
Carbonic anhydrase 2	51.62	47.49	39.22	42.64	53.03	53.65	48.18	26.41
Carboxypeptidase B2	50.19	53.3	55.71	49.04	71.82	56.12	61.97	43.01
Eukaryotic translational initiation factor 4E	37.3	40.34	44.97	54.65	46.68	51.6	53.76	41.71
Heparan sulphate glucosamine 3-O-sulfotransferase 3A1	43.76	45.09	44.65	43.65	78.9	54.62	48.1	47.98
Histone acetyltransferase KAT2A	44.25	54.84	47.54	47.97	76.47	80.13	72.29	61.2
Inositol-tetrakisphosphate 1-kinase	45.49	47.46	42.28	46.08	68.44	55.84	55.52	47.76
Lysine-specific demethylase 4C	47.58	46	54.22	47.21	65.45	58.89	70.85	44.04
Methionine aminopeptidase 1	55.43	56.44	51.82	46.12	76.33	63.55	59.14	45.68
Methionine aminopeptidase 2	46.83	48.25	45.71	40.11	43.77	54.88	30.94	23.54
Mitofusin-1	56.06	55.98	56.6	52.65	74.22	65.94	59.58	nd
NAD(P)H dehydrogenase [quinone] 1	48.01	55.78	50.22	48.23	78.42	62.74	55.66	45.84
Phosphoenolpyruvate carboxykinase, cytosolic [GTP]	49.82	46.77	50.86	41.29	67.21	50.96	63.36	43.08
Phospholipase A2, membrane associated	52.93	53.72	54.52	47.57	70.81	56.78	65.98	54.32
Polypeptide N-acetylgalactosaminyltransferase 2	59.69	57.76	56.42	51.96	76.42	66.87	65.06	56.17
Pyruvate kinase PKM	52.34	53.3	53.56	56.28	68.36	49.53	63.46	28.71
Ras-related C3 botulinum toxin substrate 1	50.34	55.33	49.56	50.44	68.85	54.05	71.79	54.26
Ras-related protein Rab7a	51.23	51.73	65.5	52	67.27	44.8	62	58.08
Serine/threonine-protein phosphatase 5	51.42	46.91	65.49	42.42	64.87	50.57	51.54	33.99
Sulfotransferase 1e4	48.97	58.29	44.49	48.16	56.55	51.19	49.17	44.1
Sulfotransferase family cytosolic 1B member 1	49.44	52.89	46.34	45.75	67.75	58.64	64.66	51.8

Scores are intended as arbitrary values (on a maximum of 100) according to the Molecular Interaction Fields (MIFs) used in the calculation. Red cells indicate a bad ligand-protein fitting; Green cells indicate medium ligand-protein fitting; Blue cells indicate a good ligand protein fitting

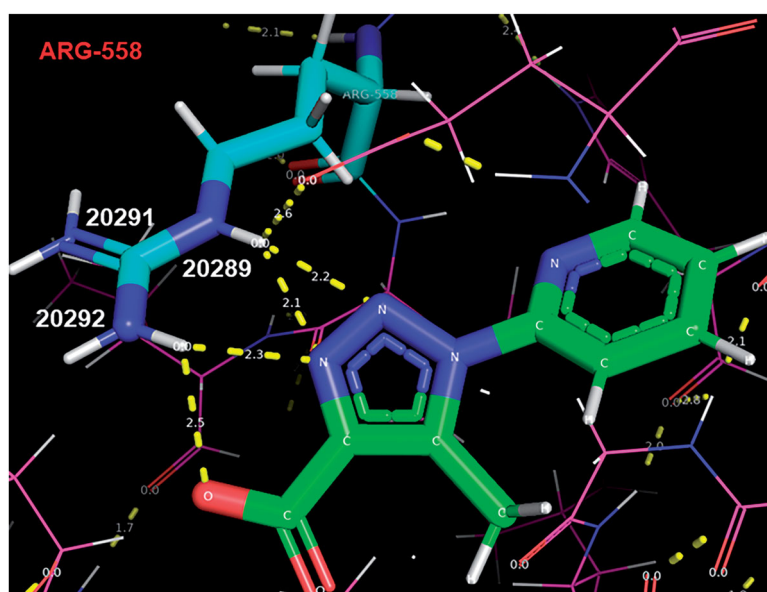


Figure 4. PyMOL outlook of triazole 16 bound to KAT2A active site pocket. Triazole's 16 nitrogens are coloured in blue, carbons in green and oxygens in red.

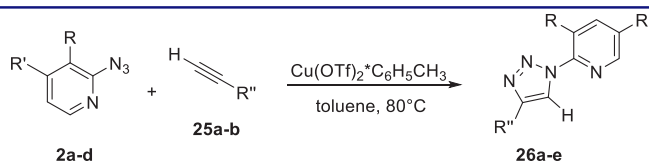
long chain acid **15** showed a good fitting with sixteen proteins (Table 1) hence lacked selectivity from the premises and for this reason was discarded. In conclusion, this dataset showed that the presence of a 5-hydroxy, or its ketol form, on the triazole generated a class of compounds that were not useful for further medicinal chemistry investigations with the 20 selected proteins. Equally, compound **17** (Table 1), showed a promiscuous behaviour with up to thirteen proteins and, therefore, was abandoned.

At this point we focussed our attention on compound **16**, which docking with KAT2A was reported to be peculiarly higher than any of the other binders **11–15** and **17,18**, reaching 80.13 (Table 1)¹. Considering that many of the known ligands for KAT2A comprise a carboxylate functionality (Figure 3), we hypothesised that the binding data for compound **16** were dependent on the presence of a carboxylic function at the C4 position which favoured the interaction of triazole **16** with the desired target (Figure 4), whereas triazole **18**, bearing an ester function at C4, showed a

lower binding score with KAT2A (Table 1). In support of our hypothesis, polar contacts connecting **16** and KAT2A occurred mainly when **16**'s OH function of the carboxylic moiety and **16**'s N2-N3 atoms of the triazole ring interacted with the NH functions of KAT2A Arg-558 residue (shown with blue and light blue sticks, Figure 4).

In particular, **16**'s N2 and N3 atoms of the triazole ring coordinate arginine NH number 20289 (2.2 Å and 2.1 Å distance respectively, Figure 4) while the N3 atom of the triazole ring and the OH function of the carboxylic moiety coordinate arginine NH number 20292 (2.3 Å and 2.5 Å distance respectively, Figure 4).

The low binding-affinity of triazole **18** with all the 20 proteins and the interactions of **16** with KAT2A identified in this work (Figure 4), clearly indicated that this selection of proteins required triazole binders to possess hydrogen-bond donor and acceptors units at C4 and C5, which may have been a discriminator in the selection of targets from the BioGPS database⁴⁶. In summary, the analysis of the docking studies identified **16** as a potential scaffold

Table 2. Synthesis of pyridyl-based triazoles **26a-e**^a.

Entry	Azide	R	R'	Alkyne	R''	Product	Yield (%) ^b
1	2a	H	H	25a	COOEt	26a	90
2	2a	H	H	25b	(CH ₂) ₄ COOH	26b	89
3	2b	OCH ₃	H	25a	COOEt	26c	78
4	2c	H	CH ₃	25a	COOEt	26d	94
5	2d	H	Cl	25a	COOEt	26e	99

^aReaction conditions: **2a-d** (1 equiv.), **25a,b** (1.1 equiv.), Cu(OTf)₂·C₆H₅CH₃ (0.1 equiv.), toluene (0.25 M).

^bIsolated yields.

to be evaluated as KAT2A inhibitor. For this reason, we proceeded with the synthesis of a small library of triazole **16** analogs **26a-e** and **27a-d**.

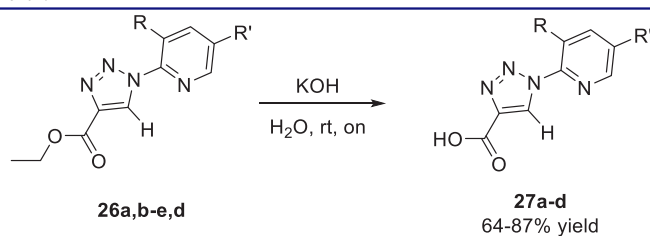
2.2. Synthesis of pyridyl-triazoles **26a-f** and **27a-d**

A small library of 1,2,3-triazoles **26a-e** and **27a-d** bearing either a carboxylate or an ester functionality at C4 was therefore prepared (Table 2). We anticipated that the carboxylic functionality was indeed crucial to high binding, however, we also noted that compound **18**, i.e., the ethyl ester of compound **16**, showed a significant binding for KAT2A. Hence, both carboxylates and their esters were included in the library.

The synthesis of compounds **26a-e** has been carried out following a procedure previously reported¹². Pyridine azides **2a-e** were reacted with alkynes **25a,b** to give triazoles **26a-e** via a CuAAC cycloaddition protocol (Table 2)⁵⁰. Pyridine-based triazoles **26a-d** were obtained in high yields (Table 2). Considering that carboxylates were found better ligands by virtual screening, as highlighted in the docking results (Table 1), we then proceeded with the hydrolysis of esters **26a,b** and **26d,e** to reveal the corresponding acids **27a-d** (Table 3). This entailed standard saponification using a solution of potassium hydroxide, which provided **27a-d** in good to high yields.

2.3. Preliminary binding studies through fluorescence analysis

The binding properties, alongside the ability of **16** and **27a-d** to inhibit the activity of KAT2A were evaluated using a standard protocol based upon the measurement of fluorescence⁵¹. KAT2A fluorogenic assay was developed by others to screen for inhibitors of this enzyme⁵². This test is based on the transfer of an acetyl group from acetyl-CoA (acetyl coenzyme A) to a peptide substrate. After incubation with acetyl-CoA and the inhibitor, the KAT2A enzyme generates acetylated histone H3 peptide and CoASH. The thiol group of CoASH can be detected with fluorescein isothiocyanate isomer I (5-FITC), which is a reliable reaction considering the reactivity towards nucleophiles including amines and sulfhydryl groups present on proteins⁵¹. The fluorescein isothiocyanate isomer I (5-FITC) absorption is at wavelength = 495 nm and emission = 525 nm. In the experiment, which relies on the measurement of emission at 525 nm, strong emissions were observed when a poor inhibition of KAT2A was realised; on the contrary, poor emissions at 525 nm indicated high levels of inhibition (Figure 5). Each assay was run in triplicate and at increasing concentrations of **16**, **26c** and **27a-d** (1.5 μM, 5 μM, 10 μM and

Table 3. Hydrolysis of triazoles **26a,b,d,e** to reveal corresponding carboxylates **27a-d**^a.

Entry	Triazole	R	R'	Product	Yield (%) ^b
1	26a	H	H	27a	87
2	26b	OCH ₃	H	27b	70
3	26d	H	CH ₃	27c	71
4	26e	H	Cl	27d	64

^aReaction conditions: **26a,b,d,e** (1 equiv.), KOH (1 equiv.), H₂O (1 M).

^bIsolated yields.

15 μM). As shown in Figure 5, compounds **27a** and **27b** displayed a good inhibitory activity at as low as 5 μM (coloured in blue) while higher concentrations were required for triazoles **16** and **26c** (15 μM, coloured in black, and 10 μM, coloured in red, respectively). Compound **27c** also displayed a good inhibition of KAT2A acetylating activity at just 5 μM concentration (coloured in blue). A significant divergence was observed for the behaviour of **27d**, which holds a *p*-Cl substitution on the pyridine ring. The results collected indicated that **27d** seemed to promote rather than inhibit the enzymatic activity of KAT2A, as highlighted by the increasing level of CoASH produced vs concentration (Figure 5). This result was most unexpected in lieu of the striking similarity between **27d** and **27a-c** and it should be looked in more details in future work.

In summary, we have demonstrated that triazoles **16**, **26c** and **27a-c** possess inhibitory activity of KAT2A whereas only **27d** proved to behave as an activator. Compounds **16**, **26c** and **27a-d** were then subjected to *in vitro* assays in a cell model displaying dysfunctional activity of KAT2A to confirm the bioactivity.

2.4. In vitro testing of triazoles **16**, **26c** and **27a-d**

Compounds **16**, **26c** and **27a-d** were tested in U937 cell line (from human myeloid leukaemia, AML) in which KAT2A is known to be overexpressed⁵³. U937 cells were stimulated with different concentrations of compounds **16**, **26c** and **27a-d**, starting from 200 μM. Cell viability was measured by thiazolyl blue tetrazolium

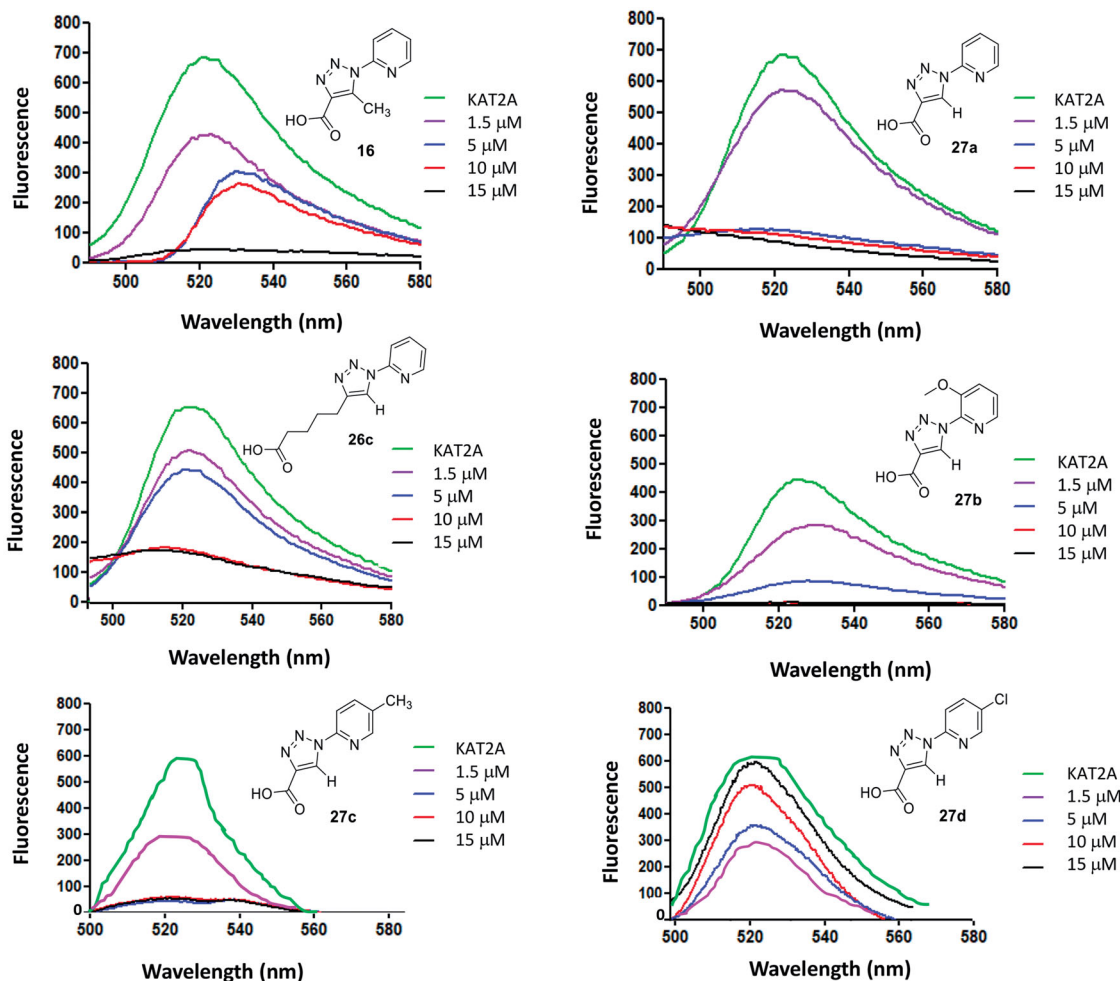


Figure 5. KAT2A fluorescence tests performed on triazoles 16, 26c and 27a-d.

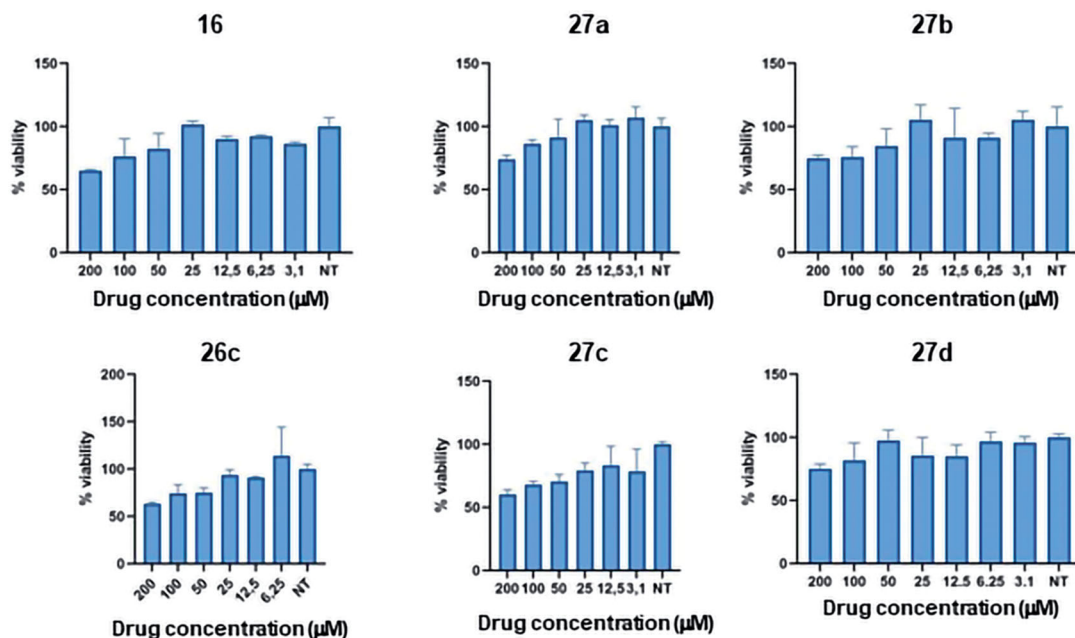


Figure 6. MTT assay performed on triazoles 16, 26c and 27a-d. NT = non treated.

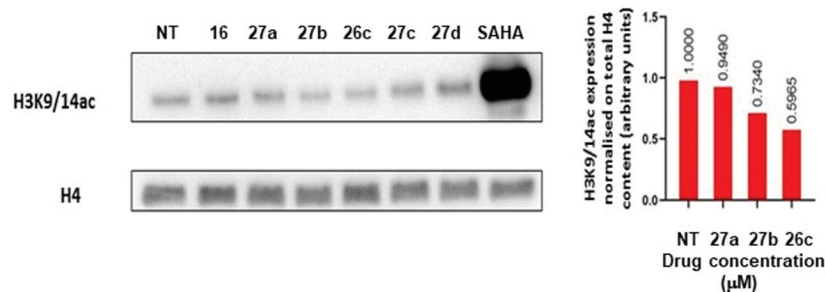


Figure 7. WB analysis (on the left) of **16**, **26c** and **27a-d** showing H3K9/14ac levels in U937 cells following 24 h treatment at the concentration of 200 μM; 5 μM SAHA treatment was used as a positive control of acetylation. Densitometric analysis of WB is shown on the right.

bromide (MTT) assay. This assay displayed a slight reduction (10–20%) in cell viability by all the compounds tested (Figure 6).

To investigate compounds **16**, **26c** and **27a-d** induced inhibition of KAT2A acetylation levels of histone H3K9/14ac were analysed. To this end, U937 cells were treated with a 200 μM concentration of compounds **16**, **26c** and **27a-d** for 24 h. SAHA (suberoylanilide hydroxamic acid), a known histone deacetylase inhibitor, was used as a positive control of acetylation at 5 μM concentration. Histone extraction and subsequent Western Blot (WB) analysis were carried out checking H3K9/14ac acetylation levels. Triazole **26c** showed 40% reduction in the acetylation of H3K9/14ac (Figure 7) which was the strongest inhibition value obtained.

Considering the results obtained, it is possible that a lateral and flexible chain at C4 on the triazole ring is required to allow a tight interaction of triazoles and KAT2A. This in addition to the presence of a hydrogen-bond acceptor site which is represented by the carboxylate function.

3. Conclusion

In conclusion, we identified a new class of binders/inhibitors of KAT2A which comprises a pyridine and a long chain carboxylate linked *via* a triazole ring. The study used virtual screening to select a small library of pyridine-based 1,2,3-triazoles, including **26a-e** and **27a-d**. We then submitted triazoles **26a-e** and **27a-d** to fluorescence binding assays versus KAT2A enzyme which confirmed the binding abilities of these entities to KAT2A. Fluorescence binding assays revealed that only triazoles **27a-d** and **26c** interacted with KAT2A, meanwhile their correspondent ester analogs **26a,b,e,f** did not show any binding. Finally, we evaluated the *in vitro* activity of **26c** and **27a-d** in U937 cell line of human AML and found out **26c** to be the most active compound showing a 40% inhibition of KAT2A acetylating activity. It is noteworthy that compound **26c**, having a longer chain, displayed the best inhibitory activity *in vitro*; meanwhile, shorter chain carboxylate, alike **16** or **27**, that were demonstrated optimal binders, showed reduced activity compared to **26c**. Studies are currently ongoing to (1) determine the structure-activity relationship (SAR) of **26c** analogs and (2) improve potency and selectivity of this new template (**26c**) for KAT2A inhibition at a lower dose concentration.

Note

1. Although the dataset predicted **16** as a good binder also for other proteins, the value of these interactions was inferior to a point that selectivity could be, at least in principle, possible.

Acknowledgements

The authors acknowledge IRC GOIPG/2018/3165 for support to RP and VALERE: “Vanvitelli per la Ricerca Program: EPInhibitDRUGre (CUP B66J20000680005) and Programma Operativo Nazionale (PON) Ricerca e Innovazione 2014–2020 AIM attrazione e mobilità dei ricercatori” for supporting NDG and GB research about KAT2A biological assays.

Disclosure statement

No potential conflict of interest was reported by the author(s).

Funding

This work was supported by Irish Research Council (GOIPG/2018/3165), Programma Operativo Nazionale Ricerca e Competitività (Ricerca e Innovazione 2014–2020 AIM), and VALERE (EPInhibitDRUGre (CUP B66J20000680005)).

ORCID

Lucia Altucci  <http://orcid.org/0000-0002-7312-5387>
 Menotti Ruvo  <http://orcid.org/0000-0001-5997-756X>
 Rosa Bellavita  <http://orcid.org/0000-0003-2163-5163>
 Paolo Grieco  <http://orcid.org/0000-0002-6854-8123>
 Mauro F. A. Adamo  <http://orcid.org/0000-0001-9072-3648>

References

1. Angell YL, Burgess K. Peptidomimetics via copper-catalyzed azide-alkyne cycloadditions. *Chem Soc Rev* 2007;36: 1674–89.
2. Kharb R, Sharma PC, Yar MS, et al. Pharmacological significance of triazole scaffold. *J Enzyme Inhib Med Chem* 2011; 26:1–21.
3. Schulze B, Schubert US. Beyond click chemistry-supramolecular interactions of 1,2,3-triazoles. *Chem Soc Rev* 2014; 43:2522–71.
4. Palmer MH, Parsons S. 4-Methyl-1,2,4-Triazole and 1-Methyl-Tetrazole. *Acta Crystallogr Sect C Cryst Struct Commun* 1996;52:2818–22.
5. Sheremet EA, Tomanov RI, Trukhin EV, Berestovitskaya VM. Synthesis of 4-aryl-5-nitro-1,2,3-triazoles. *Russ J Org Chem* 2004;40:594–5.
6. Hafez HN, Abbas HAS, El-Gazzar ARBA. Synthesis and evaluation of analgesic, anti-inflammatory and ulcerogenic

- activities of some triazolo- and 2-pyrazolyl-pyrido[2,3-d]-pyrimidines. *Acta Pharm* **2008**;58:359–78.
7. Liu K, Shi W, Cheng P. The coordination chemistry of Zn(II), Cd(II) and Hg(II) complexes with 1,2,4-triazole derivatives. *Dalton Trans* **2011**;40:8475–90.
 8. Passannanti A, Diana P, Barraja P, et al. Pyrrolo[2,3-d][1,2,3]triazoles as potential antineoplastic agents. *Heterocycles* **1998**;48:1229–35.
 9. Johns BA, Weatherhead JG, Allen SH, et al. The use of oxadiazole and triazole substituted naphthyridines as HIV-1 integrase inhibitors. Part 1: establishing the pharmacophore. *Bioorg Med Chem Lett* **2009**;19:1802–6.
 10. Shalini K, Kumar N, Drabu S, Sharma PK. Advances in synthetic approach to and antifungal activity of triazoles. *Beilstein J Org Chem* **2011**;7:668–77.
 11. Lindstedt R, Ruggiero V, Alessio VD, et al. Inhibits T cell activation by reducing Nfat nuclear residency. *Int J Immunopathol Pharmacol* **2009**;22:29–42.
 12. Pacifico R, Destro D, Gillick-Healy MW, et al. Preparation of Acidic 5-Hydroxy-1,2,3-triazoles via the Cycloaddition of Aryl Azides with β -Ketoesters. *J Org Chem* **2021**;86:11354–60.
 13. Hamada Y. Role of pyridines in medicinal chemistry and design of BACE1 inhibitors possessing a pyridine scaffold. In: Pandey PP, ed. *Pyridine*. London, UK: IntechOpen; **2018**. DOI: [10.5772/intechopen.74719](https://doi.org/10.5772/intechopen.74719)
 14. Asif M. Biological potential and chemical properties of pyridine and piperidine fused pyridazine compounds: pyridopyridazine a versatile nucleus. *Asian J Pharm Sci* **2016**;1:29.
 15. Nobeli I, Price SL, Lommerse JPM, Taylor R. Hydrogen bonding properties of oxygen and nitrogen acceptors in aromatic heterocycles. *J Comput Chem* **1997**;18:2060–74.
 16. Laurence C, Brameld KA, Graton J, et al. The pKBHX database: toward a better understanding of hydrogen-bond basicity for medicinal chemists. *J Med Chem* **2009**;52:4073–86.
 17. Kenny PW, Montanari CA, Prokopczyk IM, et al. Hydrogen bond basicity prediction for medicinal chemistry design. *J Med Chem* **2016**;59:4278–88.
 18. Eicher T, Hauptmann S, Speicher A. *The chemistry of heterocycles: structures, reactions, synthesis, and applications*. Weinheim, Germany: John Wiley & Sons; **2013**.
 19. Arnold DS, Plank CA, Erickson EE, Pike FP. Solubility of benzene in water. *J Chem Eng Data* **1958**;3:253–6.
 20. Ertl P, Rohde B, Selzer P. Fast calculation of molecular polar surface area as a sum of fragment-based contributions and its application to the prediction of drug transport properties. *J Med Chem* **2000**;43:3714–7.
 21. Hohenstein EG, Sherrill CD. Effects of heteroatoms on aromatic π - π interactions: benzene-pyridine and pyridine dimer. *J Phys Chem A* **2009**;113:878–86.
 22. Huber RG, Margreiter MA, Fuchs JE, et al. Heteroaromatic π -stacking energy landscapes. *J Chem Inf Model* **2014**;54:1371–9.
 23. Vitaku E, Smith DT, Njardarson JT. Analysis of the structural diversity, substitution patterns, and frequency of nitrogen heterocycles among U.S. FDA approved pharmaceuticals. *J Med Chem* **2014**;57:10257–74.
 24. Hsu KHK. Thirty years after isoniazid: its impact on tuberculosis in children and adolescents. *JAMA* **1984**;251:1283–5.
 25. Pym AS, Domenech P, Honoré N, et al. Regulation of catalase-peroxidase (KatG) expression, isoniazid sensitivity and virulence by furA of *Mycobacterium tuberculosis*. *Mol. Microbiol* **2001**;40:879–89.
 26. Morlock GP, Metchock B, Sikes D, et al. ethA, inhA, and katG Loci of ethionamide-resistant clinical mycobacterium tuberculosis isolates. *Antimicrob Agents Chemother* **2003**;47:3799–805.
 27. Wang Z, Vince R. Design and synthesis of dual inhibitors of HIV reverse transcriptase and integrase: introducing a dike-toacid functionality into delavirdine. *Bioorg Med Chem* **2008**;16:3587–95.
 28. Wang L, Kumar R, Pavlov PF, Winblad B. Small molecule therapeutics for tauopathy in Alzheimer's disease: walking on the path of most resistance. *Eur J Med Chem* **2021**;209:112915.
 29. Minami J, Numabe A, Andoh N, et al. Comparison of once-daily nifedipine controlled-release with twice-daily nifedipine retard in the treatment of essential hypertension. *Br J Clin Pharmacol* **2004**;57:632–9.
 30. Wang JG, Kario K, Lau T, et al. Asian Pacific Heart Association. Use of dihydropyridine calcium channel blockers in the management of hypertension in Eastern Asians: a scientific statement from the Asian Pacific Heart Association. *Hypertens Res* **2011**;34:423–30.
 31. Voss AK, Thomas T. Histone lysine and genomic targets of histone acetyltransferases in mammals. *BioEssays* **2018**;40:180078–16.
 32. Ud-Din AIMS, Tikhomirova A, Roujeinikova A. Structure and functional diversity of GCN5-related n-acetyltransferases (GNAT). *Int J Mol Sci* **2016**;17:1018.
 33. Smith BC, Denu JM. Chemical mechanisms of histone lysine and arginine modifications. *Biochim Biophys Acta Gene Regul Mech* **2009**;1789:45–57.
 34. Chen L, Wei T, Si X, et al. Lysine acetyltransferase GCN5 potentiates the growth of non-small cell lung cancer via promotion of E2F1, cyclin D1, and cyclin E1 expression. *J Biol Chem* **2013**;288:14510–21.
 35. Yin YW, Jin HJ, Zhao W, et al. The histone acetyltransferase GCN5 expression is elevated and regulated by c-Myc and E2F1 transcription factors in human colon cancer. *Gene Expr* **2015**;16:187–96.
 36. Dekker FJ, Van Den Bosch T, Martin NI. Small molecule inhibitors of histone acetyltransferases and deacetylases are potential drugs for inflammatory diseases. *Drug Discov Today* **2014**;19:654–60.
 37. Sun C, Wang M, Liu X, et al. PCAF improves glucose homeostasis by suppressing the gluconeogenic activity of PGC-1 α . *Cell Reports* **2014**;9:2250–62.
 38. Balasubramanyam K, Swaminathan V, Ranganathan A, Kundu TK. Small molecule modulators of histone acetyltransferase p300. *J Biol Chem* **2003**;278:19134–40.
 39. Arif M, Pradhan SK, Thanuja GR, et al. Mechanism of p300 specific histone acetyltransferase inhibition by small molecules. *J Med Chem* **2009**;52:267–77.
 40. Balasubramanyam K, Altaf M, Varier RA, et al. Polyisoprenylated benzophenone, garcinol, a natural histone acetyltransferase inhibitor, represses chromatin transcription and alters global gene expression. *J Biol Chem* **2004**;279:33716–26.
 41. Balasubramanyam K, Varier RA, Altaf M, et al. Curcumin, a novel p300/CREB-binding protein-specific inhibitor of acetyltransferase, represses the acetylation of histone/nonhistone proteins and histone acetyltransferase-dependent chromatin transcription. *J Biol Chem* **2004**;279:51163–71.
 42. Chimenti F, Bizzarri B, Maccioni E, et al. Novel histone acetyltransferase inhibitor modulating Gcn5 network:

- cyclopentylidene-[4-(4' chlorophenyl)thiazol-2-yl]hydrazone. *J Med Chem* **2009**;52:530–6.
43. Ghizzoni M, Haisma HJ, Dekker FJ. Reactivity of isothiazolones and isothiazolone-1-oxides in the inhibition of the PCAF histone acetyltransferase. *Eur J Med Chem* **2009**;44:4855–61.
 44. Alvarez-Sánchez R, Basketter D, Pease C, Lepoittevin JP. Studies of chemical selectivity of hapten, reactivity, and skin sensitization potency. Synthesis and studies on the reactivity toward model nucleophiles of the ¹³C-labeled skin sensitizers, 5-chloro-2-methylisothiazol-3-one (MCI) and 2-methylisothiazol. *Chem Res Toxicol* **2003**;16:627–36.
 45. Furdas SD, Shekfeh S, Bissinger EM, et al. Synthesis and biological testing of novel pyridoisothiazolones as histone acetyltransferase inhibitors. *Bioorg Med Chem* **2011**;19:3678–89.
 46. Siragusa L, Cross S, Baroni M, et al. BioGPS: navigating biological space to predict polypharmacology, off-targeting, and selectivity. *Proteins* **2015**;83:517–32.
 47. Baroni M, Cruciani G, Sciabola S, et al. A common reference framework for analyzing/comparing proteins and ligands. Fingerprints for Ligands and Proteins (FLAP): theory and application. *J Chem Inf Model* **2007**;47:279–94.
 48. Davies JP, Cotter PD, Ioannou YA. Cloning and mapping of human Rab7 and Rab9 cDNA sequences and identification of a Rab9 pseudogene. *Genomics* **1997**;41:131–4.
 49. Hinds TD, Sánchez ER. Protein phosphatase 5. *Int J Biochem Cell Biol* **2008**;40:2358–62.
 50. Rostovtsev VV, Green LG, Fokin VV, Sharpless KB. A stepwise Huisgen cycloaddition process: Copper(I)-catalyzed regioselective “ligation” of azides and terminal alkynes. *Angew Chem Int Ed* **2002**;41:2596–9.
 51. Chaganti LK, Venkatakrisnan N, Bose K. An efficient method for FITC labelling of proteins using tandem affinity purification. *Biosci Rep* **2018**;38:1–8.
 52. <https://westbioscience.com/acetyltransferase/assay-kit/gcn5-fluorogenic-assay-kit-3372.html>
 53. Kikuchi H, Kuribayashi F, Kiwaki N, et al. GCN5 regulates the superoxide-generating system in leukocytes via controlling Gp91-phox gene expression. *J Immunol* **2011**;186:3015–22.